THE JOURNAL OF BIOLOGICAL CHEMISTRY VOL. 287, NO. 27, pp. 22948–22958, June 29, 2012

Oncogenic Kras Expression in Postmitotic Neurons Leads to S100A8-S100A9 Protein Overexpression and Gliosis*[S]

Received for publication, February 29, 2012, and in revised form, May 10, 2012 Published, JBC Papers in Press, May 10, 2012, DOI 10.1074/jbc.M112.357772

Myung-Jeom Ryu[‡], Yangang Liu[‡], Xiaofen Zhong[§], Juan Du[‡], Nicholas Peterson[¶], Guangyao Kong[‡], Hongda Li[§‖], Jinyong Wang[‡], Shahriar Salamat[**], Qiang Chang[§‖], and Jing Zhang[‡1]

From the [‡]McArdle Laboratory for Cancer Research, University of Wisconsin-Madison, Madison, Wisconsin 53706, the [§]Waisman Center, University of Wisconsin-Madison, Madison, Wisconsin 53705, the [¶]Department of Biochemistry, University of Wisconsin School of Letters and Science, Madison, Wisconsin 53705, the [**]Department of Pathology and Laboratory Medicine, University of Wisconsin-Madison, Madison, Wisconsin 53792, and the [‖]Departments of Medical Genetics and Neurology, University of Wisconsin-Madison, Madison, Wisconsin 53706

Background: Hyperactivation of Ras signaling in neurons promotes gliosis and astrocytoma in a cell nonautonomous manner.
Results: Neuronal expression of Kras G12D/+ leads to gliosis and overexpression of S100A8-S100A9, which serve as chemoattractants for microglia and growth factors for astrocytes.
Conclusion: Overexpression of S100A8-S100A9 in neurons is an early event in Kras G12D-induced gliosis.
Significance: S100A8-S100A9 expressed in nonhematopoietic cells may be involved in early stage tumorigenesis.

Previous studies suggest that up-regulation of Ras signaling in neurons promotes gliosis and astrocytoma formation in a cell nonautonomous manner. However, the underlying mechanisms remain unknown. To address this question, we generated compound mice (LSL Kras G12D/+;CamKII-Cre) that express oncogenic Kras from its endogenous locus in postmitotic neurons after birth. These mice developed progressive gliosis, which is associated with hyperactivation of Ras signaling pathways. Microarray analysis identified S100A8 and S100A9 as two secreted molecules that are significantly overexpressed in mutant cortices. In contrast to their usual predominant expression in myeloid cells, we found that overexpression of S100A8 and S100A9 in the mutant cortex is primarily in neurons. This neuronal expression pattern is associated with increased infiltration of microglia in mutant cortex. Moreover, purified S100A8-S100A9 but not S100A8 or S100A9 alone promotes growth of primary astrocytes *in vitro* through both TLR4 and receptor of advanced glycation end product receptors. In summary, our results identify overexpression of S100A8-S100A9 in neurons as an early step in oncogenic Kras-induced gliosis. These molecules expressed in nonhematopoietic cells may be involved in tumorigenesis at a stage much earlier than what has been reported previously.

Pilocytic astrocytoma (PA),[2] a low grade glioma (WHO grade I), is the second most common brain tumor found in children (1). These tumors may arise anywhere within the neuroaxis and are generally composed of neoplastic glial fibrillary acidic protein (GFAP)-positive cells (2). The earlier observation that one-third of PA tumors arise in children with the neurofibromatosis type 1 (NF1) implicates the involvement of the *NF1* gene in the molecular pathogenesis of PA (3). *NF1* encodes a GTPase-activating protein (GAP) of p21 RAS proteins, which accelerates the intrinsic hydrolysis of RAS-GTP to RAS-GDP and the conversion of Ras from its active GTP-bound form to an inactive GDP-bound form (4). Consistent with the role of Nf1 as a RAS-GAP (a negative regulator of Ras signaling), loss of Nf1 expression in various cell types is associated with higher levels of activated Ras (Ras-GTP) and increased Ras downstream signaling in both human and mouse (5–11), whereas overexpression of the GAP domain of Nf1 leads to reduction of Ras hyperactivation to wild-type levels (12). These studies implicate the possible involvement of oncogenic *RAS* in PA development. Indeed, subsequent studies identified mutations in the *KRAS* gene in ~5% of sporadic NF1-free PA patients (1, 13).

Extensive research has been focusing on how dysregulated Ras signaling leads to PA. Ablation of Nf1 expression in neurons results in severe reactive gliosis in mouse, indicating a cell-nonautonomous role of neurons in gliosis, a condition involved in many diseases of the central nervous system (*e.g.* inflammation and stroke) (14). However, these mice show no evidence of neurofibromas or optic pathway gliomas (a subtype of PA) that are common features of human NF1 (15). These data indicate that although *Nf1*-deficient neurons promote proliferation/survival of wild-type glial cells, they are insufficient to generate gliomas. Astrocyte-specific knock-out of Nf1

* This work was supported, in whole or in part, by National Institutes of Health Grants R01 CA152108 and P30 CA014520-UW Comprehensive Cancer Center Support from the NCI. This work was also supported by a Howard Temin Award, a Shaw Scientist Award from the Greater Milwaukee Foundation, a V Scholar Award from the V Foundation for Cancer Research, an Investigator Initiated Grant from University of Wisconsin Carbone Comprehensive Cancer Center (to J. Z.), and a Postdoctoral Fellowship from the American Heart Association (to M. J.).
[S] This article contains supplemental Figs. S1–S5 and Materials and Methods.
[1] To whom correspondence should be addressed. Tel.: 608-263-1147; Fax: 608-262-2824; E-mail: zhang@oncology.wisc.edu.

[2] The abbreviations used are: PA, pilocytic astrocytoma; RAGE, receptor of advanced glycation end products; GFAP, glial fibrillary acidic protein; P1, postnatal day 1; GAP, GTPase-activating protein.

in mice leads to preferential hyperactivation of Kras but not other Ras isoforms (12). Astrocyte-specific expression of endogenous oncogenic Kras (Kras G12D) (12) or astrocyte-specific inactivation of Nf1 (16) results in moderate gliosis but does not lead to PA. However, in combination with germ line removal of one copy of Nf1, these genetic alterations result in optic pathway gliomas (12, 17). These results suggest that although dysregulated Ras signaling in astrocytes alone (either through loss of Nf1 or expression of oncogenic Kras) is insufficient to generate gliomas, these astrocytes in the presence of *Nf1* heterozygous neurons might be able to generate gliomas. It is likely that neurons with dysregulated Ras signaling secrete growth factors/chemokines that support proliferation and/or survival of adjacent astrocytes and thus promote gliosis and gliomas.

S100A8 and S100A9 are predominantly expressed and secreted by myeloid cells, including granulocytes, monocytes, myeloid-derived suppressor cells, and other immature cells of myeloid lineage (18, 19). They belong to a family of more than 20 EF-hand motif calcium-binding proteins in vertebrates. Secreted S100A8-S100A9 are reported to bind to Toll-like receptor 4 (TLR4) and receptor of advanced glycation end products (RAGE) and play an important role in anti-infection, autoimmunity, and cancer (18, 19). Under inflammatory conditions as well as in many tumors, the expression levels of S100A8 and S100A9 are significantly up-regulated. Recent studies show that S100A8-S100A9 not only serve as markers of immune cells within the tumor microenvironment, but they also play independent pathogenic roles in cancer progression and metastasis. However, up-regulation of S100A8-S100A9 expression in nonhematopoietic cells and their involvement in early stage tumorigenesis have not been reported before.

Here, we use a mouse model that expresses endogenous oncogenic Kras in post-mitotic neurons since postnatal day 1 (P1) to study the molecular mechanisms underlying how dysregulated Ras signaling in neurons leads to gliosis, a process involving neuron-to-astrocyte signaling that may be important for astrocytoma formation. Our results identify S100A8 and S100A9 as major players mediating this process. These molecules are predominantly overexpressed in mutant neurons and can directly promote astrocyte growth *in vitro* through both RAGE and TLR4 receptors. Increased infiltration of microglia in the mutant cortex might also contribute to the gliosis phenotype. Our study identifies elevated expression of S100A8 and S100A9 in neurons as an early and key step in oncogenic Kras-induced gliosis and suggests a potential role of these molecules in pre-cancer or early stage tumorigenesis.

MATERIALS AND METHODS

Mice—The LSL Kras G12D/+ mice (20) were crossed to CamKII-Cre transgenic mice (21, 22) to generate mice carrying both alleles (*LSL Kras G12D/+;CamKII-Cre*). All mouse lines were maintained on a pure C57BL/6 genetic background (>N10). All experiments were conducted with the ethical approval of International Association for Assessment and Accreditation of Laboratory Animal Care at the University of Wisconsin-Madison.

Microarray Analysis—Total RNAs were isolated from the cortices of four pairs of mutants and their littermate controls (17–19 weeks old). Microarray was performed using the whole mouse genome array (4X44K; Agilent Technologies). Statistical analysis of the obtained data were performed using Edge[3] software (23) to identify differentially expressed genes. The identified significantly up-regulated genes were sorted into biological pathways using DAVID functional analyses (24, 25).

Western Blot Analysis—Preparation of protein lysates from cortices and analysis of Western blot were performed essentially as described previously (26). Briefly, the cortex regions were isolated from the whole brain, rinsed with PBS, and sonicated in lysis buffer containing 7 M urea, 2 M thiourea, 4% CHAPS, 130 mM dithiothreitol, a complete protein inhibitor mixture (Roche Applied Science), and 1 mM NaF and Na_2VO_3. Protein lysates were resolved on 4–12% polyacrylamide gels (Novex) in MOPS buffer. The primary antibodies against the following antigens were used in this study: GFAP (1:1000; Millipore), S100A8 and S100A9 (10 μg/ml; R & D Systems), α-actin (1:5000; Sigma), IκBβ (1:2000; Santa Cruz Biotechnology), and ERK, p-ERK, Akt, p-Akt, p85/70S6K, and p-p85/70S6K (1:1000; Cell Signaling Technologies). Protein expression levels were quantified using ImageQuant software (GE Healthcare) and normalized against their respective controls.

Immunofluorescence Staining—Free-floating sections were cut at 40 μm on a freezing microtome. Primary antibodies were used against GFAP (1:1000; Millipore) or Ki67 (1:500; DAKO) and followed by Cy2- or Cy3-conjugated secondary antibodies (Jackson ImmunoResearch). Slides were counterstained with DAPI (Vector Laboratories) and mounted in Fluoromount G (Electron Microscopy Sciences). The sections were examined using fluorescence microscopy (Zeiss).

Semi-quantitative RT-PCR—Total RNAs were isolated from dissected cortices using RNeasy mini kit (Qiagen). First strand cDNAs were synthesized using random primers and SuperScriptII reverse transcriptase (Invitrogen). The PCRs were performed under the following conditions: 94 °C for 2 min, 34 cycles at 94 °C for 30 s, 60 °C for 30 s, and 72 °C for 30 s. Primers used for RT-PCR were as follows: 5′-TGAGCAACCTCATTGATGTCTACC-3′ (forward) and 5-ATGCCACACCCACTTTTATCACC-3′ (reverse) for mS100A8; 5′-TCATCGACACCTTTCCATCAA-3′ (forward) and 5′-GATCAATGCCATCAGCA-3′ (reverse) for mS100A9. The PCR products were quantified using ImageQuant software (GE Healthcare) and normalized against GAPDH.

Isolation and Analysis of Myeloid Cells—Mice were perfused with Hanks' balanced salt solution before cortex or whole brain dissection. Microglia/macrophages were enriched using Percoll gradient centrifugation from homogenized tissue essentially as described previously (27, 28). The enriched viable cells were counted in 0.4% trypan blue (Sigma). The isolated cells were stained simultaneously with allophycocyanin (APC)-conjugated antibody against Mac1 (M1/70), phycoerythrin (PE)-conjugated antibody against CD45 (30-F11), and fluorescein isothiocyanate (FITC)-conjugated antibody against Gr-1 (RB6–8C5). All antibodies were purchased from eBiosciences. The stained cells were analyzed on a FAC-

SCalibur (BD Biosciences). The data were analyzed using FlowJo Version 9.0.2 software (Version 1.0.2, TreeStar).

Immunohistochemistry—Paraffin sections were cut at 5 μm, deparaffinized, and rehydrated. The color visualization of the primary antibodies was performed with either the SuperSensitive^{TM} polymer-HRP IHC Detection System (for GFAP, Iba1, and NeuN; BioGenex) or Vectastain Elite ABC kit (for S100A8 and S100A9; Vector Laboratories) according to the manufacturer's instructions. Slides were counterstained with hematoxylin and mounted with Permount. The primary antibodies against following antigens were used in this study: GFAP (1:1000; Millipore), Iba1 (1:200; Wako), NeuN (1:1000; Millipore), S100A8 (1:50; Santa Cruz Biotechnology), and S100A9 (5 μg/ml; R&D Systems). The sections were examined using bright field microscopy (Leica).

Purification of S100A8 and S100A9 Proteins—S100A8 and S100A9 were amplified from wild-type mouse spleen. The PCR products were cloned into the pFC-14K HaloTag T7 Flexi vector (Promega). Recombinant S100A8-Halo and S100A9-Halo proteins were purified using HaloLink resin (Promega), and the HaloTag was removed via proteolytic cleavage using HaloTEV protease (Promega) according to the manufacturer's instructions. Purified proteins were separated by SDS-PAGE and stained with Coomassie Blue to confirm their purities.

Primary Cell Cultures—Cortices were isolated from wild-type mice on postnatal day 1, dissociated, and cultured for neurons (Neurobasal medium (Invitrogen) containing B27, glutamine, and penicillin/streptomycin) or astrocytes (DMEM containing 1% FBS and penicillin/streptomycin) essentially as described (29). 500 live astrocytes were seeded in triplicate in 96-well plates in the presence of vehicle or various concentrations of purified S100A8 and/or S100A9. To block the function of S100A8-S100A9 receptors, cells were treated with 50 ng/ml rat IgG2a (isotype control for TLR4 antibody), goat IgG (isotype control for RAGE antibody), TLR4 blocking antibody (clone MTS510, eBioscience) (30), or RAGE blocking antibody (R&D) (31) for 1 h prior to the addition of vehicle or 50 ng/ml of purified S100A8-S100A9. After 96 h in culture, numbers of viable cells were determined using CellTiter Glo Assay (Promega) according to the manufacturer's instructions.

To visualize cultured astrocytes, 2500 live cells were seeded on polylysine (Sigma)-coated coverslips in 24-well plates and cultured in the presence of S100A8-S100A9 (50 ng/ml) or vehicle. After 96 h in culture, cells were fixed with 4% paraformaldehyde and permeabilized with 0.3% Triton X-100 in PBS. Immunofluorescence staining for GFAP was performed as described above.

RESULTS

Kras G12D/+ Mutant Cortex Displays a Progressive Gliosis—To induce expression of oncogenic Kras in postmitotic neurons, we bred conditional oncogenic *Kras* mice (Lox-Stop-Lox-[LSL] Kras G12D/+) (20) with CamKII-Cre transgenic mice (21, 22) to generate compound mice (*LSL Kras G12D/+;CamKII-Cre*) on a pure C57BL/6 background. We refer to these compound mice as Kras G12D/+ mice and CamKII-Cre mice as wild-type control mice throughout.

To determine whether neuronal expression of endogenous oncogenic Kras leads to gliosis, we examined GFAP expression in forebrain, midbrain, and hindbrain from 8-week-old control and Kras G12D/+ mutant mice using Western blot analysis (supplemental Fig. S1). Only mutant forebrain showed significant up-regulation of GFAP compared with controls. Thus, we focused on the cortex for further characterization. As expected, the GFAP level in mutant cortex was significantly elevated (~3-fold compared with control cortex) (Fig. 1*A*). To confirm that the increased GFAP level in mutant cortex is due to increased number of GFAP-positive astrocytes, we performed GFAP immunofluorescence staining on serially sectioned control and mutant cortices (Fig. 1*B*). Kras G12D/+ mutant mice displayed extensive GFAP immunoreactivity, which reflects gliosis throughout the cerebral cortex. Our result is consistent with a previous report that loss of NF1 function in neurons induces reactive gliosis in the brain (14). Further analysis with simultaneous staining of Ki67 and GFAP detected no appreciable level of proliferation in these GFAP$^+$ astrocytes in the cortex (Fig. 1*C*). As a positive control, Ki67 immunoreactivity was readily detected in neural stem/progenitor cells in both the subventricular zone and the subgranular zone on the same section.

Because mutant neurons express oncogenic Kras since postnatal day 1 (P1), we analyzed control and mutant mice at different ages to determine the onset of gliosis in mutant cortex (Table 1). Three of three 4-week-old Kras G12D/+ mice showed indistinguishable GFAP immunoreactivity from control mice, whereas 4/5 8- and 3/3 15-week-old mutant mice displayed strong GFAP immunoreactivity compared with controls. Our results indicate that Kras G12D/+ cortex develops a progressive gliosis. However, none of the mutant mice developed astrocytoma. Furthermore, to determine whether this gliosis phenotype is associated with neuronal degeneration, we examined Kras G12D/+ cortices for evidence of necrosis or apoptosis using H&E and caspase 3 staining and were unable to detect evidence of degenerating neurons. These results suggest that expression of Kras G12D/+ in neurons might alter normal neuronal physiology and thus exerts an effect on surrounding astrocytes (14, 32, 33).

Neuronal Expression of Kras G12D/+ Promotes Hyperactivation of Multiple Downstream Signaling Pathways in Mutant Cortex—To investigate whether expression of endogenous oncogenic Kras in neurons promotes aberrant downstream signaling in the mutant cortex, we first examined the well characterized Ras effector pathways, PI3K/Akt and MEK/ERK, in lysates prepared from freshly isolated control and mutant cortices (Fig. 2, *A* and *B*). As expected, both pathways were hyperactivated in mutant cortices. Consistent with this result, the level of phospho-S6K, a convergent target of the Akt and ERK pathways, was also significantly elevated in mutant cortices (Fig. 2*C*). It was previously shown that NFκB is activated by oncogenic Ras (34, 35), and activation of the NFκB pathway is required for oncogenic *Kras*-induced lung tumorigenesis (36). Thus, we examined the expression level of IκBβ, a negative regulator of the NFκB pathway, in control and mutant cortices and found that IκBβ was down-regulated in Kras G12D/+ cortex (Fig. 2*D*). Taken together, these results indicate that neuro-

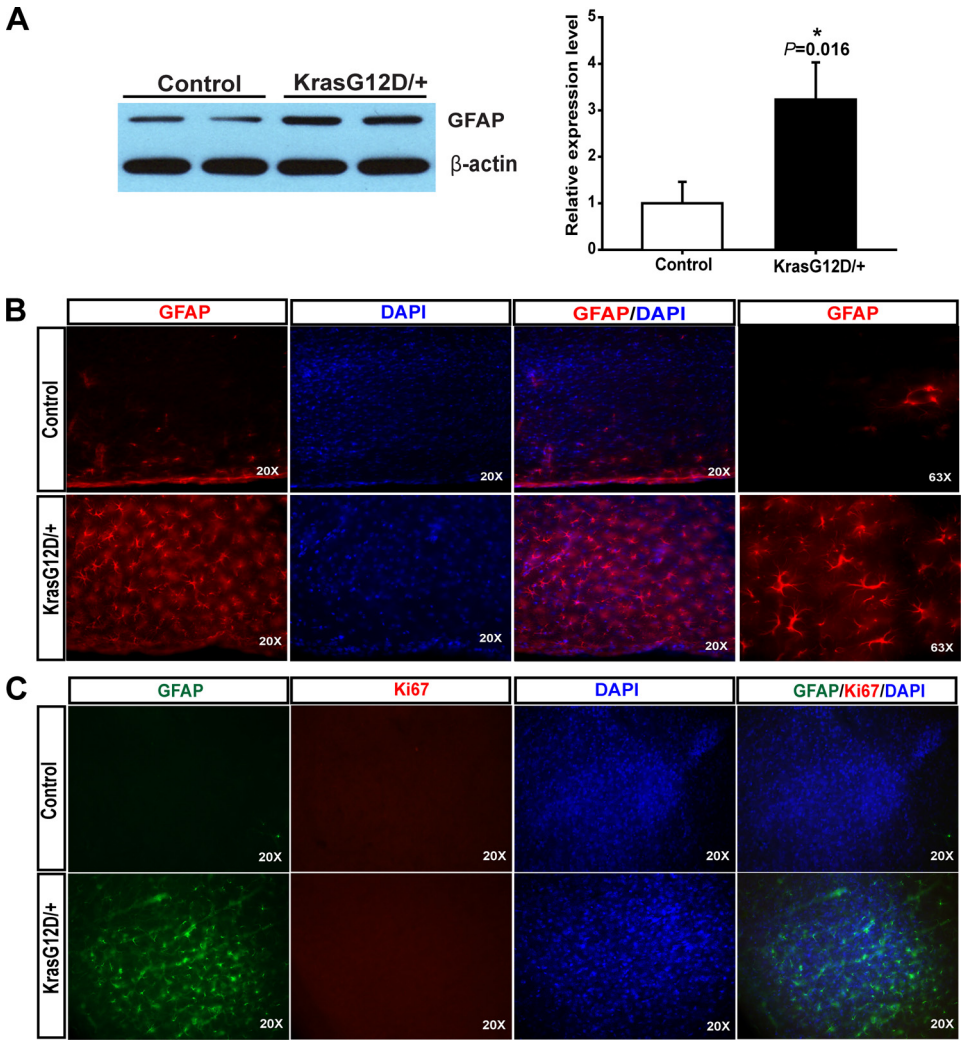

FIGURE 1. **Neuronal expression of endogenous Kras G12D induces gliosis.** In compound CamKII-Cre; LSL Kras G12D/+ (Kras G12D/+) mice, expression of endogenous Kras G12D was induced in postmitotic neurons since P1. *A,* expression levels of GFAP were analyzed by Western blot using protein extracts from cortices of 8-week-old control and Kras G12D/+ mice. GFAP levels relative to β-actin levels in Kras G12D/+ cortices were quantified and compared with those in control cortices ($n = 4$). The average of control is arbitrarily set at 1. Results are presented as average + S.D. *Asterisk* indicates statistically significant change. *B* and *C,* representative images of coronal sections (40 μm thickness, Cryostat) of the cortices stained with GFAP antibodies (*red*) and DAPI (*blue*) or (*B*) GFAP antibodies (*green*), Ki67 antibodies (*red*), and DAPI (*blue*) (*C*).

TABLE 1

CamKII-Cre;KrasG12D/+ mice develop a progressive gliosis

+++, strong expression; ++, moderate expression; -, no expression.

Age	Genotypes	GFAP immunostaining
4 weeks	Control ($n = 2$)	-
	CamKII-Cre;KrasG12D/+ ($n = 3$)	-
8 weeks	Control ($n = 3$)	-
	CamKII-Cre;KrasG12D/+ ($n = 5$)	+++ (4/5), ++ (1/5)
15 weeks	Control ($n = 2$)	-
	CamKII-Cre;KrasG12D/+ ($n = 3$)	+++

nal expression of oncogenic Kras indeed elicits profound signaling changes in the mutant cortex, and these changes might contribute to gliosis.

S100A8 and S100A9 Are Significantly Overexpressed in Kras G12D/+ Neurons—Because hyperactivation of Ras signaling is often associated with overproduction of secreted proteins (37), we hypothesized that Kras G12D neurons provide additional growth factors that support proliferation and/or survival of adjacent astrocytes, which subsequently leads to gliosis. To identify such potential growth factors, we examined gene transcription profiles in four pairs of control and mutant cortices using Agilent two-color microarray analysis. The significantly dysregulated genes were further analyzed to identify genes encoding known or unknown secreted proteins. S100A8 and S100A9 were found as two of the most up-regulated genes encoding secreted proteins in a mutant cortex (Fig. 3*A*). This microarray result was further validated using semi-quantitative RT-PCR at the RNA level (Fig. 3*B*) and Western blot analysis at the protein level (Fig. 3*B*).

Because S100A8 and S100A9 are primarily expressed in myeloid cells (18), for example, neutrophils, monocytes, and tissue-infiltrated macrophages, we were wondering which cell type(s) overexpresses them in the Kras G12D/+ cortex. Three major cell types could be readily labeled in a mutant cortex using immunohistochemical staining as follows: NeuN for neurons, GFAP for astrocytes, and Iba1 for microglia (Fig. 4*A*). We found that in Kras G12D/+ cortices, both S100A8 and S100A9 were predominantly overexpressed in neurons (Fig. 4*B*), supporting our initial hypothesis.

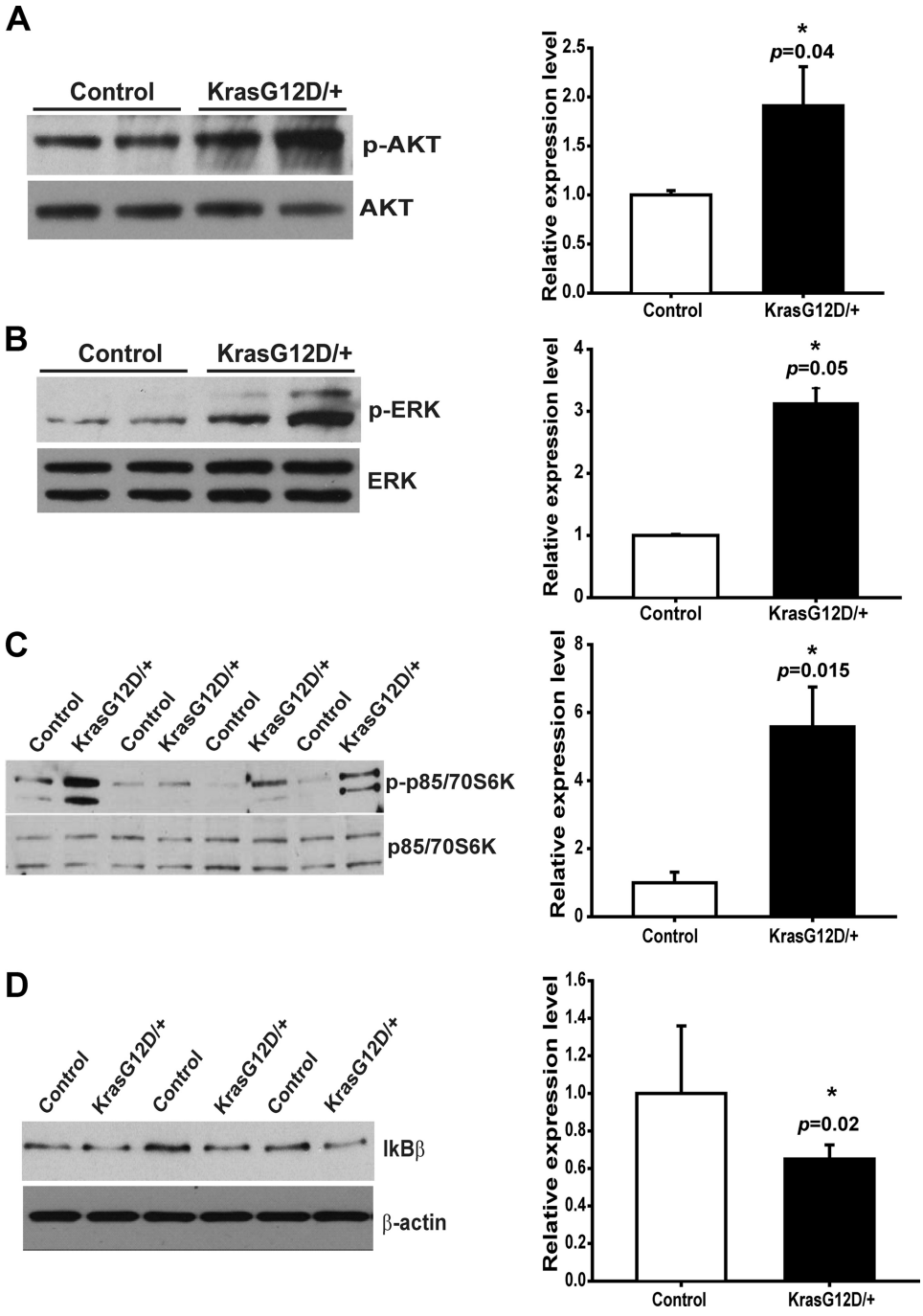

FIGURE 2. **Ras signaling pathways are hyperactivated in Kras G12D/+ cortex.** Protein lysates were prepared from 12- to 18-week-old control and CamKII-Cre; LSL Kras G12D/+ (*Kras G12D/+*) cortices. Activation of multiple signaling pathways downstream of Kras was measured by Western blot. The averages of controls are arbitrarily set at 1. Results are presented as average + S.D. *Asterisks* indicate statistically significant changes. *A–C,* phosphorylated and total levels of Akt (*A, n* = 3), ERK (*B, n* = 3), and p85/70S6K (*C, n* = 4) proteins were measured by Western blot. Phosphorylated protein levels relative to their total protein levels in Kras G12D/+ cortices were quantified and compared with those in control cortices. *D,* expression levels of IκBβ, a negative regulator of NF-κB signaling, relative to β-actin levels in Kras G12D/+ cortices were quantified and compared with those in control cortices (*n* = 3).

Kras G12D/+ Cortex Shows Increased Infiltration of Myeloid Cells—Several studies show that S100A8 and S100A9 act as strong chemoattractants for monocytes and neutrophils (38–41). Therefore, we further analyzed microglia and macrophages in control and mutant cortices to determine whether overexpression of S100A8 and S100A9 in mutant neurons is correlated to increased infiltration of these cells. Immunohistochemical staining of Iba1 displayed that in some areas of mutant cortex the number of microglia appeared significantly increased (supplemental Fig. S2).

To accurately quantify the number of infiltrated myeloid cells in control and mutant cortices, these cells were enriched and analyzed using flow cytometry (Fig. 5) (27, 28). The total number of recovered myeloid cells was significantly increased in mutant cortices compared with that in control cortices (~2-fold increase of $Mac1^+$ cells, M; Fig. 5*B*). Further fractionation

A

Gene Name	Access. No.	Fold change (KrasG12D/control) Pair 1	Pair 2	Pair 3	Pair 4
S100A8	NM_013650	4.98	3.65	2.73	7.23
S100A9	NM_009114	3.89	3.42	8.03	5.26

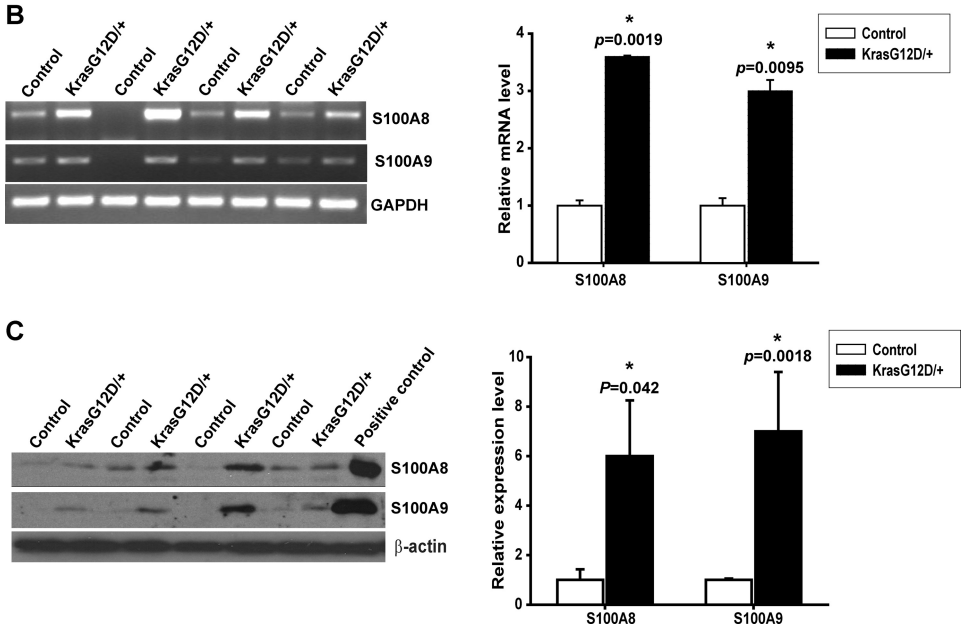

FIGURE 3. **S100A8 and S100A9 are overexpressed in Kras G12D/+ cortex.** *A,* expression level changes of S100A8 and S100A9 in four pairs of control and CamKII-Cre; LSL Kras G12D/+ (Kras G12D/+) cortices (17–19 weeks old) using Agilent mouse whole-genome microarray analysis ($p < 0.01$). *B* and *C,* validation of microarray results by semi-quantitative RT-PCR (*B*) and Western blot (*C*). The averages of controls are arbitrarily set at 1. Results are presented as average + S.D. *Asterisks* indicate statistically significant changes. *B,* S100A8 or S100A9 mRNA levels relative to GAPDH levels in Kras G12D/+ cortices were quantified and compared with those in control cortices ($n = 4$). *C,* S100A8 or S100A9 protein levels relative to β-actin levels in Kras G12D/+ cortices were quantified and compared with those in control cortices ($n = 4$).

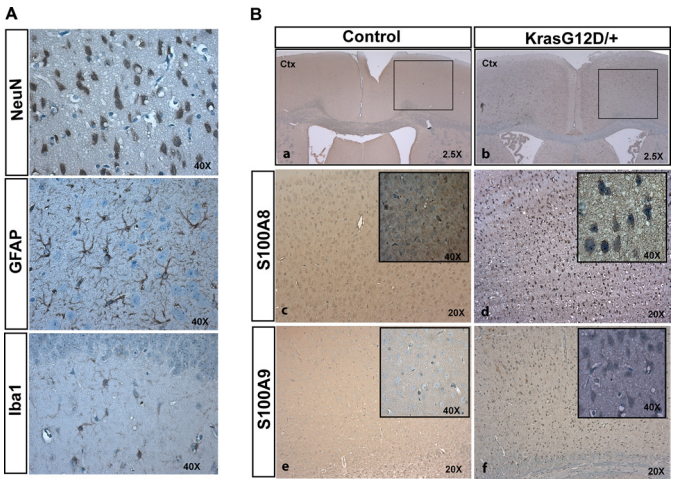

FIGURE 4. **S100A8 and S100A9 are overexpressed in Kras G12D/+ neurons.** Cortices were isolated from 12-week-old control and CamKII-Cre; LSL Kras G12D/+ (Kras G12D/+) mice ($n = 3$). Serial coronal sections were cut at 5 μm thickness (paraffin) and analyzed by NeuN, GFAP, Iba1, S100A8, and S100A9 immunohistochemical staining. *A,* representative images of NeuN, GFAP, and Iba1 immunoreactivities to show the morphologies of neurons, astrocytes, and microglia, respectively, in Kras G12D/+ cortex. *B,* immunohistochemical analysis of S100A8 and S100A9 in control and Kras G12D/+ cortex. *Panels c* and *d,* high magnification views of the *boxed area* in *panels a* and *b*. The *insets* in *panels c–f* show high magnification views of cells overexpressing S100A8 in *panels c* and *d* or S100A9 in *panels e* and *f*. Morphologically, S100A8- or S100A9-positive cells resemble neurons. *Ctx,* cerebral cortex.

of recovered myeloid cells showed that the number of microglia ($Mac1^+$ $CD45^{mid}$, R2; Fig. 5*A*) (42) was moderately increased in mutant cortices (~2.2-fold over controls), although the numbers of macrophages ($Mac1^+$ $CD45^{hi}$, R1; Fig. 5*A*) (42) and neutrophils ($Mac1^+$ $Gr1^{hi}$, M1; Fig. 5*B*) were much more elevated in mutant cortices compared with those in controls (above 4-fold increase). To determine whether increased myeloid cells in Kras G12D/+ cortices is caused by overproduction of these cells in blood, we performed a complete blood count in a large cohort of control and Kras G12D/+ mice, and no such evidence was found (Table 2). Rather, our results suggest that increased infiltration of microglia/macrophages and neutrophils in mutant cortices might be mediated through chemokines (including S100A8 and S100A9) produced by Kras G12D/+ neurons.

Purified S100A8-S100A9 Promotes Primary Astrocyte Growth in Vitro Partially through the TLR4 and RAGE Receptors—To test whether S100A8 and S100A9 can exert any direct effects on astrocytes, we first examined whether these cells express the receptors for S100A8 and S100A9, TLR4 (43), and/or RAGE (44). Indeed, both TLR4 and RAGE were readily detectable in cultured primary astrocytes using RT-PCR (supplemental Fig. S3). We then purified S100A8 and S100A9 from transiently transfected 293T cells using HaloTag purification system (Fig. 6*A*). When primary astrocytes were cultured in the presence of these exogenous factors, we found that only S100A8-S100A9, but not S100A8 alone or S100A9 alone, pro-

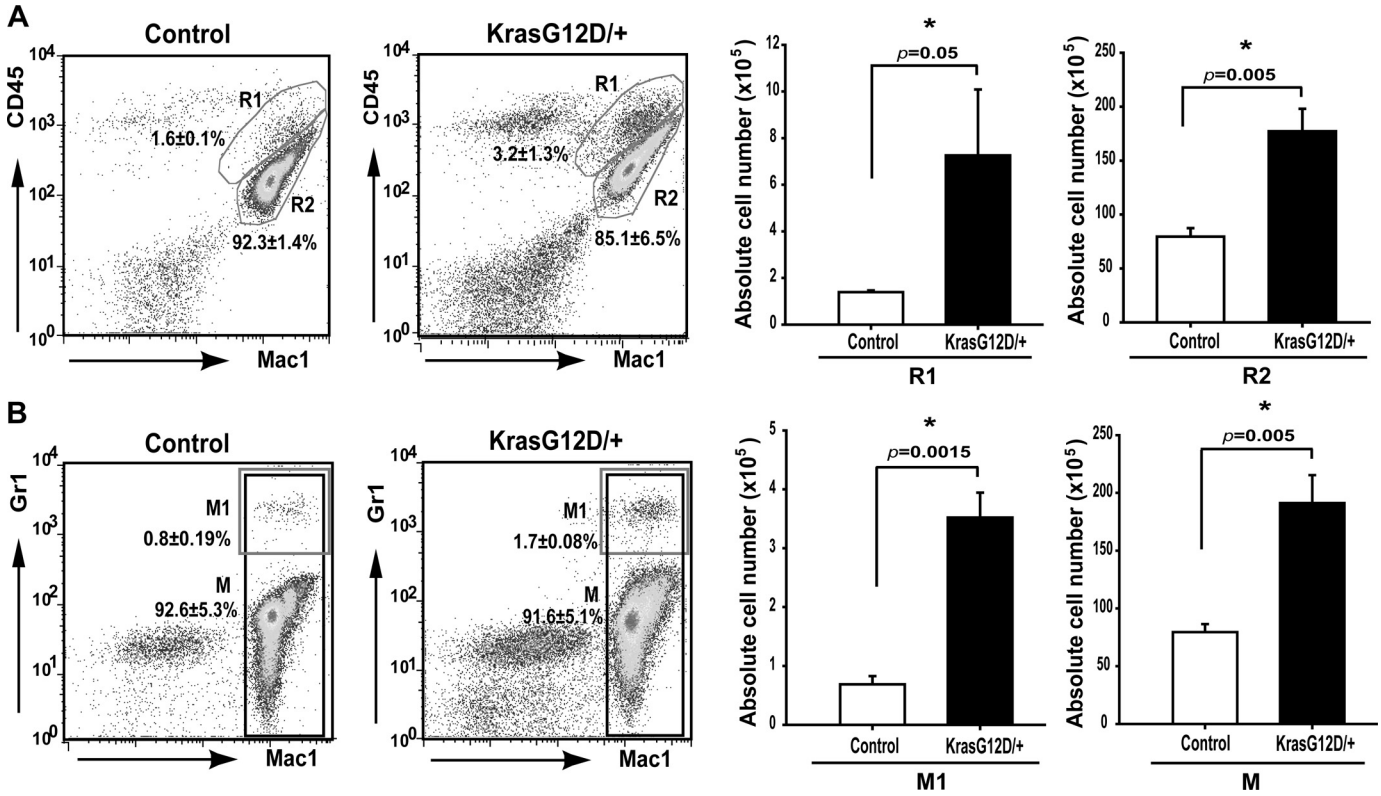

FIGURE 5. **Myeloid cells accumulate in Kras G12D/+ cortex.** Twelve-week-old control and CamKII-Cre; LSL Kras G12D/+ (Kras G12D/+) mice ($n = 3$) were perfused with Hanks' balanced salt solution before cortex dissection. Microglia/macrophages were enriched using Percoll gradient centrifugation from homogenized cortex. Numbers of purified live cells were counted. Flow cytometric analysis and quantification of different populations of myeloid cells were performed in enriched cells. Different populations of myeloid cells and their percentages are indicated on representative density plots. The absolute numbers of purified live cells are presented in *bar graphs*. Results are presented as average + S.D. *Asterisks* indicate statistically significant changes. *A,* flow cytometric analysis and quantification of macrophage ($Mac1^+$ $CD45^{hi}$, R1) and microglia ($Mac1^+$ $CD45^{mid}$, R2). *B,* flow cytometric analysis and quantification of neutrophils ($Mac1^+$ $Gr1^{hi}$, M1) and total myeloid cells ($Mac1^+$, M).

TABLE 2

Complete blood count analysis of CamKII-Cre;KrasG12D/+ and control mice

The *p* value is 0.06, 0.14, 0.27, and 0.2 for WBC, hematocrit, platelet, and RBC, respectively.

	WBC (× 10^3 per μl)		Hematocrit		Platelet (× 10^3 per μl)		RBC (× 10^6 per μl)	
Genotype	Range	Median	Range	Median	Range	Median	Range	Median
			%					
Control ($n = 10$)	3.2–8.8	6.5	42–47.6	44	898–1290	1141	8.66–9.88	9.23
KrasG12D/+ ($n = 12$)	2–11.8	9	38.6–66.4	46	838–1592	1175	7.96–13.26	9.31

moted astrocyte growth in a dose-dependent manner (Fig. 6*B*). Further examination of cultured astrocytes in the presence of S100A8-S100A9 not only validated increased cell numbers as shown in CellTiter Glo assay (Fig. 6*B*) but also demonstrated up-regulation of GFAP compared with vehicle control (Fig. 6*C*). These effects are consistent with the phenotypes we observed *in vivo*, suggesting that neuronal expression of endogenous Kras G12D induces gliosis mainly through up-regulating S100A8-S100A9 expression.

To determine whether S100A8-S100A9 promotes astrocyte growth through the known TLR4 and/or RAGE receptors, we cultured primary astrocytes with 50 ng/ml of S100A8-S100A9 and in the presence of isotype control antibodies, TLR4 blocking antibody, or RAGE blocking antibody over a wide range of concentrations (50–200 ng/ml) (Fig. 6*D*). Both of these blocking antibodies efficiently inhibited astrocyte growth promoted by S100A8-S100A9.

Purified S100A8-S100A9 Does Not Directly Activate Peripheral Blood Monocytes/Macrophages—We tested whether S100A8-S100A9 directly activates monocytes/macrophages (supplemental Fig. S4). Peripheral blood monocytes/macrophages were incubated with or without 1 μg/ml LPS (serving as a positive control) or 50 ng/ml purified S100A8-S100A9. Upon LPS stimulation, production of TNFα was observed in ~55% of monocytes/macrophases, a hallmark of monocyte/macrophage activation. However, production of TNFα in these cells incubated with S100A8-S100A9 was comparable with that in unstimulated cells, indicating that S100A8-S100A9 does not directly activate monocytes/macrophages.

DISCUSSION

In this work, we study the molecular mechanisms underlying gliosis induced by Kras G12D/+ neurons. First, expression of endogenous Kras G12D/+ in postmitotic neurons after birth

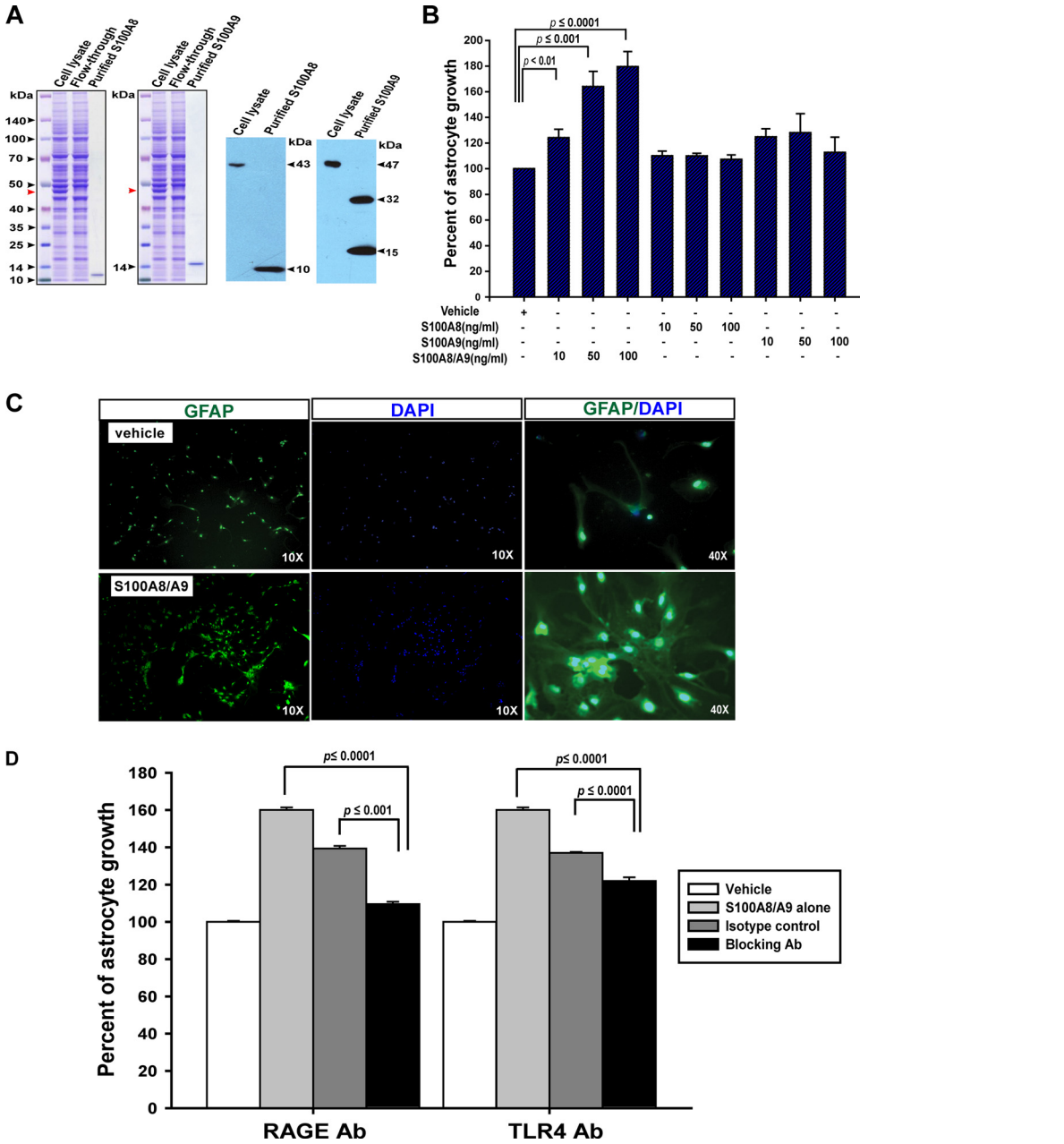

FIGURE 6. **S100A8-S100A9 complex promotes astrocyte growth *in vitro* partially through the TLR4 and RAGE receptors.** *A,* purification of mouse S100A8 and S100A9 proteins from transiently transfected HEK293T cells. *Left panels,* Coomassie Blue-stained SDS-polyacrylamide gels show purification of mS100A8 and mS100A9 proteins using the HaloTag purification system. *Cell lysate* represents the total protein extracts from transiently transfected HEK292T cells; *flow-through* represents the unbound lysate after an overnight incubation with HaloLink resin, and purified proteins are the tag-free mS100A8 and mS100A9 proteins after HaloTag-TEV protease cleavage of the HaloLink resin. *Red arrowheads* indicated the mS100A8-Halo or mS100A9-Halo overexpressed in HEK293T cells. *Right panels,* Western blot analysis of S100A8 and S100A9 confirms the identities of purified proteins. Note: minor fraction of mS100A9 was purified as homodimers, similar to purified hS100A9 in other reports. *B, C,* and *D,* cortices were isolated from wild-type P1 neonates and dissociated. Cells were cultured *in vitro* to promote astrocyte growth. Confluent astrocytes were split and seeded in triplicate in 96-well plates. Astrocytes were cultured for 96 h before analyses. *B,* cell viability was analyzed by CellTiter Glo assay. Percentages of astrocyte growth in response to S100A8 alone, S100A9 alone, or S100A8-S100A9 complex were quantified relative to vehicle control, which is arbitrarily set at 100%. Results are presented as average + S.D. ($n = 5$). *C,* representative images of GFAP staining (*green*) in wild-type astrocytes cultured in the presence of 100 ng/ml S100A8-S100A9 complex or vehicle. The cell nuclei were counterstained with DAPI (*blue*). *D,* astrocyte cultures were set up as described under "Materials and Methods." Cell viability was analyzed by CellTiter Glo assay. Percentages of astrocyte growth in response to S100A8-S100A9 alone or S100A8-S100A9 with different isotype controls or blocking antibodies were quantified relative to vehicle control, which is arbitrarily set at 100%. Results are presented as average + S.D. ($n = 3$).

induces a progressive gliosis but not astrocytoma. Second, overexpression of S100A8 and S100A9 in mutant neurons correlates with increased infiltration of microglia and other myeloid cells in mutant cortex. These cells might partially contribute to the gliosis phenotype. Third, purified S100A8-S100A9 but not S100A8 or S100A9 alone promotes primary astrocyte growth *in vitro* through both RAGE and TLR4 receptors.

Neuronal Expression of Endogenous Kras G12D/+ Induces a Progressive Gliosis but Not Astrocytoma—Gliosis often occurs in response to infection, injury, or neurodegeneration. Under

these conditions, astrocytes in the central nervous system undergo hypertrophy, which is associated with altered gene expression, including up-regulation of GFAP (45). One postmortem case study reported three NF1 patients with extensive astrogliosis (46), suggesting that in the case of dysregulated Ras signaling gliosis might reflect a pre-cancer stage. The development of progressive gliosis in our model (Fig. 1 and Table 1) is consistent with that observed in the $NF1^{SynI}KO$ mice, in which Nf1 expression is specifically ablated in neurons (14). However, we do not observe the cortical compression phenotype reported in $NF1^{SynI}KO$ mice. This difference is likely due to the different temporal expression of the Cre recombinase. Synapsin I-Cre drives Nf1 loss in neurons as early as embryonic day 12.5 (14), although CamKII-Cre induces Kras G12D expression since P1 (21, 22). In addition, because the spatial patterns of Cre recombinase are different between these two Cre lines, gliosis is observed primarily in the cerebral cortex in our model (supplemental Fig. S1), although it is most severe in the brainstem in the $NF1^{SynI}KO$ mice (14). Because our model involves the expression of Kras G12D in all forebrain neurons, it might not recapitulate gliosis occurring under a physiological condition of infection, injury, or neurodegeneration, which only involves local or a group of neurons.

Gliosis in the $NF1^{SynI}KO$ mice is not associated with extensive neuronal death or microgliosis (14). In our model, although we did not observe any evidence of neurodegeneration, increased infiltration of microglia and other types of myeloid cells to the mutant cortex is evident (Fig. 5). Because it is well documented that microglia play an important role in inflammatory diseases of the brain as well as in brain tumors (42), increased infiltration of microglia in the Kras G12D/+ cortex might partially contribute to the gliosis phenotype. In addition to the different temporal and spatial expression patterns of Cre lines used in two studies, the difference in signaling strength elicited by the loss of Nf1 and the expression of Kras G12D might also attribute to the distinct involvement of microglia in gliosis. Biochemically, NF1 inactivation is a less severe lesion than an oncogenic Ras mutation because oncogenic Ras mutations impair both endogenous Ras GTPase activities and the association of Ras proteins with Ras GAP proteins, whereas NF1 abolishes its interaction with Ras proteins without affecting their GTPase activities. In addition, NF1 is only one of more than 20 Ras GAP proteins found in mammals. It is likely that its inactivation is partially compensated by other family members. Conceivably, the Ras-GTP level might be lower in cells deficient in NF1 than in cells expressing endogenous oncogenic Kras. This possibility is further supported by studies in the hematopoietic system from us and other groups, which show that the myeloproliferative phenotypes induced by oncogenic Kras are much more severe than those initiated by NF1 deficiency (47–49).

The absence of astrocytoma in our model is not surprising because previous studies suggest that dysregulation of Ras signaling in only one cell type, either in neurons or astrocytes, is insufficient to cause astrocytoma (12, 14, 16). Rather, these genetic alterations in astrocytes in combination with germ line removal of one copy of Nf1 result in optic pathway gliomas (12, 17), suggesting that more than one cell type is required in brain tumorigenesis. Thus, neural stem cells that can generate both neurons and astrocytes become an attractive candidate to initiate astrocytomas. The role of neural stem cells in astrocytoma development has been validated by the findings that concomitant deletion of p53 and PTEN or expression of Kras G12D in neural stem cells leads to highly penetrant astrocytoma (50, 51). Nonetheless, our model of postmitotic neuron-specific expression of oncogenic Kras allows us a unique opportunity to study neuron-to-astrocyte signaling that may be important for astrocytoma formation. Indeed, gene set enrichment analysis of our microarray results reveals that glioma-associated genes are significantly enriched among genes differentially expressed in the Kras G12D mutant cortex.

S100A8 and S100A9 Play Dual Functions in Kras G12D-induced Gliosis—Our data suggest that S100A8 and S100A9 act as both growth factors to promote primary astrocyte growth and chemokines to induce the infiltration of myeloid cells to the cortex, consistent with the dual role of these molecules in inflammation-associated cancer (52). The growth-promoting activity of S100A8-S100A9 on various human cancer cells was previously documented (31, 53). This activity was mediated by RAGE. Consistent with this finding, we found that primary astrocytes express RAGE (supplemental Fig. S3). Interestingly, after S100A8-S100A9 binds to RAGE, multiple signaling pathways are activated, including Ras/ERK/NFκB and PI3K/Akt (31, 44, 53). Thus, it is possible that the profound signaling changes we observed in the Kras G12D/+ cortex (Fig. 2) are caused by a combination of neuronal expression of Kras G12D and overexpression of S100A8-S100A9. However, in contrast to previous studies, S100A8-S100A9 promotes astrocyte growth at a concentration in the range of nanograms/ml (Fig. 6*B*) rather than micrograms/ml, more consistent with their role as growth factors. Moreover, unlike their effect on human cancer cells, the growth-promoting activity of S100A8-S100A9 on astrocytes is through both RAGE and TLR4 receptors (Fig. 6*D*).

The observed increased infiltration of microglia and other types of myeloid cells in the mutant cortex (Fig. 5) could be caused by elevated myeloid cells in the peripheral blood of mutant mice. We think this is unlikely, because the complete blood cell count in mutants is indistinguishable from that of wild-type control (Table 2). Alternatively, Kras G12D/+ neurons may secret chemotactic factors to attract more myeloid cells. Indeed, several studies have reported that S100A8 and S100A9 act as strong chemoattractants for monocytes and neutrophils (38–41) as well as for metastatic lung cancer cells (54). Thus, it is possible that S100A8 and S100A9 overexpressed/secreted by the Kras G12D/+ neurons serve as chemokines to attract monocytes and neutrophils.

A Model for Kras G12D/+ Neuron-induced Gliosis—Based on our data, we propose the following model to explain neuronal expression of Kras G12D-induced gliosis (supplemental Fig. S5). When postmitotic neurons express Kras G12D from its endogenous locus after birth, expression levels of S100A8 and S100A9 are significantly elevated. Secreted S100A8-S100A9 may act as chemoattractants for myeloid cells (*e.g.* monocytes and neutrophils). The increased infiltration of these cells in turn might regulate mutant neurons and wild-type astrocytes in

the mutant cortex. Over time, significant overexpression of S100A8-S100A9 potentially promotes astrocyte growth and eventually leads to severe gliosis. This model will be tested in future studies using genetic approaches.

Acknowledgments—We are grateful to Drs. David A. Tuveson and Tyler Jacks for providing us the conditional oncogenic Kras mice. We thank Drs. Lara Collier, John Kuo, Albee Messing, and John Svaren for helpful discussion and critical comments on the manuscript. We are grateful to Dr. Megan L. Derezinski for help with IbaI staining and Dr. Saeid Ghavamid for suggestions of blocking antibodies. We thank the University of Wisconsin Carbone Comprehensive Cancer Center for use of its Shared Services to complete this research.

REFERENCES

1. Sharma, M. K., Zehnbauer, B. A., Watson, M. A., and Gutmann, D. H. (2005) RAS pathway activation and an oncogenic RAS mutation in sporadic pilocytic astrocytoma. *Neurology* **65,** 1335–1336
2. Gutmann, D. H. (2008) Using neurofibromatosis-1 to better understand and treat pediatric low grade glioma. *J. Child Neurol.* **23,** 1186–1194
3. Gutmann, D. H., Donahoe, J., Brown, T., James, C. D., and Perry, A. (2000) Loss of neurofibromatosis 1 (NF1) gene expression in NF1-associated pilocytic astrocytomas. *Neuropathol. Appl. Neurobiol.* **26,** 361–367
4. Xu, G. F., O'Connell, P., Viskochil, D., Cawthon, R., Robertson, M., Culver, M., Dunn, D., Stevens, J., Gesteland, R., White, R., *et al.* (1990) The neurofibromatosis type 1 gene encodes a protein related to GAP. *Cell* **62,** 599–608
5. Basu, T. N., Gutmann, D. H., Fletcher, J. A., Glover, T. W., Collins, F. S., and Downward, J. (1992) Aberrant regulation of ras proteins in malignant tumorcells from type 1 neurofibromatosis patients. *Nature* **356,** 713–715
6. DeClue, J. E., Papageorge, A. G., Fletcher, J. A., Diehl, S. R., Ratner, N., Vass, W. C., and Lowy, D. R. (1992) Abnormal regulation of mammalian p21ras contributes to malignant tumor growth in von Recklinghausen (type 1) neurofibromatosis. *Cell* **69,** 265–273
7. Sherman, L. S., Atit, R., Rosenbaum, T., Cox, A. D., and Ratner, N. (2000) Single cell Ras-GTP analysis reveals altered Ras activity in a subpopulation of neurofibroma Schwann cells but not fibroblasts. *J. Biol. Chem.* **275,** 30740–30745
8. Lau, N., Feldkamp, M. M., Roncari, L., Loehr, A. H., Shannon, P., Gutmann, D. H., and Guha, A. (2000) Loss of neurofibromin is associated with activation of RAS/MAPK and PI3-K/AKT signaling in a neurofibromatosis 1 astrocytoma. *J. Neuropathol. Exp. Neurol.* **59,** 759–767
9. Bollag, G., Clapp, D. W., Shih, S., Adler, F., Zhang, Y. Y., Thompson, P., Lange, B. J., Freedman, M. H., McCormick, F., Jacks, T., and Shannon, K. (1996) Loss of NF1 results in activation of the Ras signaling pathway and leads to aberrant growth in hematopoietic cells. *Nat. Genet.* **12,** 144–148
10. Largaespada, D. A., Brannan, C. I., Jenkins, N. A., and Copeland, N. G. (1996) Nf1 deficiency causes Ras-mediated granulocyte/macrophage colony-stimulating factor hypersensitivity and chronic myeloid leukemia. *Nat. Genet.* **12,** 137–143
11. Hiatt, K. K., Ingram, D. A., Zhang, Y., Bollag, G., and Clapp, D. W. (2001) Neurofibromin GTPase-activating protein-related domains restore normal growth in $Nf1^{-/-}$ cells. *J. Biol. Chem.* **276,** 7240–7245
12. Dasgupta, B., Li, W., Perry, A., and Gutmann, D. H. (2005) Glioma formation in neurofibromatosis 1 reflects preferential activation of K-RAS in astrocytes. *Cancer Res.* **65,** 236–245
13. Janzarik, W. G., Kratz, C. P., Loges, N. T., Olbrich, H., Klein, C., Schäfer, T., Scheurlen, W., Roggendorf, W., Weiller, C., Niemeyer, C., Korinthenberg, R., Pfister, S., and Omran, H. (2007) Further evidence for a somatic KRAS mutation in a pilocytic astrocytoma. *Neuropediatrics* **38,** 61–63
14. Zhu, Y., Romero, M. I., Ghosh, P., Ye, Z., Charnay, P., Rushing, E. J., Marth, J. D., and Parada, L. F. (2001) Ablation of NF1 function in neurons induces abnormal development of cerebral cortex and reactive gliosis in the brain. *Genes Dev.* **15,** 859–876
15. Riccardi, V. M. (1999) in *Neurofibromatosis: Phenotypes, Natural History, and Pathogenesis* (Friedman, J. M., Gutmann, D. H., MacCollin, M., and Riccardi, V. M., eds) pp. 1–25, John Hopkins Press, Baltimore, MD
16. Bajenaru, M. L., Zhu, Y., Hedrick, N. M., Donahoe, J., Parada, L. F., and Gutmann, D. H. (2002) Astrocyte-specific inactivation of the neurofibromatosis 1 gene (NF1) is insufficient for astrocytoma formation. *Mol. Cell. Biol.* **22,** 5100–5113
17. Bajenaru, M. L., Hernandez, M. R., Perry, A., Zhu, Y., Parada, L. F., Garbow, J. R., and Gutmann, D. H. (2003) Optic nerve glioma in mice requires astrocyte Nf1 gene inactivation and Nf1 brain heterozygosity. *Cancer Res.* **63,** 8573–8577
18. Ghavami, S., Chitayat, S., Hashemi, M., Eshraghi, M., Chazin, W. J., Halayko, A. J., and Kerkhoff, C. (2009) S100A8-S100A9. A Janus-faced molecule in cancer therapy and tumorigenesis. *Eur. J. Pharmacol.* **625,** 73–83
19. Gebhardt, C., Németh, J., Angel, P., and Hess, J. (2006) S100A8 and S100A9 in inflammation and cancer. *Biochem. Pharmacol.* **72,** 1622–1631
20. Tuveson, D. A., Shaw, A. T., Willis, N. A., Silver, D. P., Jackson, E. L., Chang, S., Mercer, K. L., Grochow, R., Hock, H., Crowley, D., Hingorani, S. R., Zaks, T., King, C., Jacobetz, M. A., Wang, L., Bronson, R. T., Orkin, S. H., DePinho, R. A., and Jacks, T. (2004) Endogenous oncogenic K-ras(G12D) stimulates proliferation and widespread neoplastic and developmental defects. *Cancer Cell* **5,** 375–387
21. Fan, G., Beard, C., Chen, R. Z., Csankovszki, G., Sun, Y., Siniaia, M., Biniszkiewicz, D., Bates, B., Lee, P. P., Kuhn, R., Trumpp, A., Poon, C., Wilson, C. B., and Jaenisch, R. (2001) DNA hypomethylation perturbs the function and survival of CNS neurons in postnatal animals. *J. Neurosci.* **21,** 788–797
22. Rios, M., Fan, G., Fekete, C., Kelly, J., Bates, B., Kuehn, R., Lechan, R. M., and Jaenisch, R. (2001) Conditional deletion of brain-derived neurotrophic factor in the postnatal brain leads to obesity and hyperactivity. *Mol. Endocrinol.* **15,** 1748–1757
23. Vollrath, A. L., Smith, A. A., Craven, M., and Bradfield, C. A. (2009) EDGE(3). A web-based solution for management and analysis of Agilent two-color microarray experiments. *BMC Bioinformatics* **10,** 280
24. Huang da, W., Sherman, B. T., and Lempicki, R. A. (2009) Systematic and integrative analysis of large gene lists using DAVID bioinformatics resources. *Nat. Protoc.* **4,** 44–57
25. Dennis, G., Jr., Sherman, B. T., Hosack, D. A., Yang, J., Gao, W., Lane, H. C., and Lempicki, R. A. (2003) DAVID. Database for annotation, visualization, and integrated discovery. *Genome Biol.* **4,** P3
26. Ryu, M. J., Kim, D., Kang, U. B., Kim, J., Shin, H. S., Lee, C., and Yu, M. H. (2007) Proteomic analysis of γ-butyrolactone-treated mouse thalamus reveals dysregulated proteins upon absence seizure. *J. Neurochem.* **102,** 646–656
27. Cardona, A. E., Huang, D., Sasse, M. E., and Ransohoff, R. M. (2006) Isolation of murine microglial cells for RNA analysis or flow cytometry. *Nat. Protoc.* **1,** 1947–1951
28. Pino, P. A., and Cardona, A. E. (2011) Isolation of brain and spinal cord mononuclear cells using percoll gradients. *J. Vis. Exp.* **48,** 2348
29. McCarthy, K. D., and de Vellis, J. (1980) Preparation of separate astroglial and oligodendroglial cell cultures from rat cerebral tissue. *J. Cell Biol.* **85,** 890–902
30. González-Navajas, J. M., Fine, S., Law, J., Datta, S. K., Nguyen, K. P., Yu, M., Corr, M., Katakura, K., Eckman, L., Lee, J., and Raz, E. (2010) TLR4 signaling in effector $CD4^+$ T cells regulates TCR activation and experimental colitis in mice. *J. Clin. Invest.* **120,** 570–581
31. Ghavami, S., Rashedi, I., Dattilo, B. M., Eshraghi, M., Chazin, W. J., Hashemi, M., Wesselborg, S., Kerkhoff, C., and Los, M. (2008) S100A8-S100A9 at low concentration promotes tumor cell growth via RAGE ligation and MAP kinase-dependent pathway. *J. Leukocyte Biol.* **83,** 1484–1492
32. Kraig, R. P., Dong, L. M., Thisted, R., and Jaeger, C. B. (1991) Spreading depression increases immunohistochemical staining of glial fibrillary acidic protein. *J. Neurosci.* **11,** 2187–2198
33. Steward, O., Torre, E. R., Tomasulo, R., and Lothman, E. (1991) Neuronal activity up-regulates astroglial gene expression. *Proc. Natl. Acad. Sci. U.S.A.* **88,** 6819–6823
34. Finco, T. S., Westwick, J. K., Norris, J. L., Beg, A. A., Der, C. J., and Baldwin, A. S., Jr. (1997) Oncogenic Ha-Ras-induced signaling activates NF-κB transcriptional activity, which is required for cellular transformation.

J. Biol. Chem. **272,** 24113–24116
35. Mayo, M. W., Wang, C. Y., Cogswell, P. C., Rogers-Graham, K. S., Lowe, S. W., Der, C. J., and Baldwin, A. S., Jr. (1997) Requirement of NF-κB activation to suppress p53-independent apoptosis induced by oncogenic Ras. *Science* **278,** 1812–1815
36. Bassères, D. S., Ebbs, A., Levantini, E., and Baldwin, A. S. (2010) Requirement of the NF-κB subunit p65/RelA for K-Ras-induced lung tumorigenesis. *Cancer Res.* **70,** 3537–3546
37. Mathias, R. A., Chen, Y. S., Wang, B., Ji, H., Kapp, E. A., Moritz, R. L., Zhu, H. J., and Simpson, R. J. (2010) Extracellular remodeling during oncogenic Ras-induced epithelial-mesenchymal transition facilitates MDCK cell migration. *J. Proteome Res.* **9,** 1007–1019
38. Lackmann, M., Rajasekariah, P., Iismaa, S. E., Jones, G., Cornish, C. J., Hu, S., Simpson, R. J., Moritz, R. L., and Geczy, C. L. (1993) Identification of a chemotactic domain of the pro-inflammatory S100 protein CP-10. *J. Immunol.* **150,** 2981–2991
39. Devery, J. M., King, N. J., and Geczy, C. L. (1994) Acute inflammatory activity of the S100 protein CP-10. Activation of neutrophils *in vivo* and *in vitro*. *J. Immunol.* **152,** 1888–1897
40. Hobbs, J. A., May, R., Tanousis, K., McNeill, E., Mathies, M., Gebhardt, C., Henderson, R., Robinson, M. J., and Hogg, N. (2003) Myeloid cell function in MRP-14 (S100A9) null mice. *Mol. Cell. Biol.* **23,** 2564–2576
41. Roth, J., Vogl, T., Sunderkötter, C., and Sorg, C. (2003) Chemotactic activity of S100A8 and S100A9. *J. Immunol.* **171,** 5651
42. Watters, J. J., Schartner, J. M., and Badie, B. (2005) Microglia function in brain tumors. *J. Neurosci. Res.* **81,** 447–455
43. Ehrchen, J. M., Sunderkötter, C., Foell, D., Vogl, T., and Roth, J. (2009) The endogenous Toll-like receptor 4 agonist S100A8-S100A9 (calprotectin) as innate amplifier of infection, autoimmunity, and cancer. *J. Leukocyte Biol.* **86,** 557–566
44. Hermani, A., De Servi, B., Medunjanin, S., Tessier, P. A., and Mayer, D. (2006) S100A8 and S100A9 activate MAP kinase and NF-κB signaling pathways and trigger translocation of RAGE in human prostate cancer cells. *Exp. Cell Res.* **312,** 184–197
45. Ridet, J. L., Malhotra, S. K., Privat, A., and Gage, F. H. (1997) Reactive astrocytes. Cellular and molecular cues to biological function. *Trends Neurosci.* **20,** 570–577
46. Nordlund, M. L., Rizvi, T. A., Brannan, C. I., and Ratner, N. (1995) Neurofibromin expression and astrogliosis in neurofibromatosis (type 1) brains. *J. Neuropathol. Exp. Neurol.* **54,** 588–600
47. Braun, B. S., Tuveson, D. A., Kong, N., Le, D. T., Kogan, S. C., Rozmus, J., Le Beau, M. M., Jacks, T. E., and Shannon, K. M. (2004) Somatic activation of oncogenic Kras in hematopoietic cells initiates a rapidly fatal myeloproliferative disorder. *Proc. Natl. Acad. Sci. U.S.A.* **101,** 597–602
48. Le, D. T., Kong, N., Zhu, Y., Lauchle, J. O., Aiyigari, A., Braun, B. S., Wang, E., Kogan, S. C., Le Beau, M. M., Parada, L., and Shannon, K. M. (2004) Somatic inactivation of Nf1 in hematopoietic cells results in a progressive myeloproliferative disorder. *Blood* **103,** 4243–4250
49. Zhang, J., Wang, J., Liu, Y., Sidik, H., Young, K. H., Lodish, H. F., and Fleming, M. D. (2009) Oncogenic Kras-induced leukemogenesis. Hematopoietic stem cells as the initial target and lineage-specific progenitors as the potential targets for final leukemic transformation. *Blood* **113,** 1304–1314
50. Alcantara Llaguno, S., Chen, J., Kwon, C. H., Jackson, E. L., Li, Y., Burns, D. K., Alvarez-Buylla, A., and Parada, L. F. (2009) Malignant astrocytomas originate from neural stem/progenitor cells in a somatic tumor suppressor mouse model. *Cancer Cell* **15,** 45–56
51. Abel, T. W., Clark, C., Bierie, B., Chytil, A., Aakre, M., Gorska, A., and Moses, H. L. (2009) GFAP-Cre-mediated activation of oncogenic K-ras results in expansion of the subventricular zone and infiltrating glioma. *Mol. Cancer Res.* **7,** 645–653
52. Németh, J., Stein, I., Haag, D., Riehl, A., Longerich, T., Horwitz, E., Breuhahn, K., Gebhardt, C., Schirmacher, P., Hahn, M., Ben-Neriah, Y., Pikarsky, E., Angel, P., and Hess, J. (2009) S100A8 and S100A9 are novel nuclear factor-κB target genes during malignant progression of murine and human liver carcinogenesis. *Hepatology* **50,** 1251–1262
53. Ichikawa, M., Williams, R., Wang, L., Vogl, T., and Srikrishna, G. (2011) S100A8-S100A9 activate key genes and pathways in colon tumor progression. *Mol. Cancer Res.* **9,** 133–148
54. Hiratsuka, S., Watanabe, A., Aburatani, H., and Maru, Y. (2006) Tumor-mediated up-regulation of chemoattractants and recruitment of myeloid cells predetermines lung metastasis. *Nat. Cell Biol.* **8,** 1369–1375